

“Self-Immolative” Spacer for Uncaging with Fluorescence Reporting**

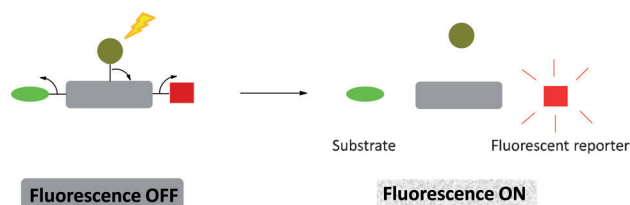
Raphaël Labruère, Ahmed Alouane, Thomas Le Saux, Isabelle Aujard, Philippe Pelupessy, Arnaud Gautier, Sylvie Dubruille, Frédéric Schmidt,* and Ludovic Jullien*

The spatio-temporal delivery of known amounts of chemicals is of major importance in chemistry, biology, and medicine. Pipettes and syringes are used in various macro- and micro-formats to fulfill this goal. However, they are intrusive and rely on convective motion, which may be detrimental to delivery to embedded and fragile samples, such as targeted cells in a living organism. Activating the release of a desired compound from an inactive precursor by introducing a non-invasive trigger (e.g., ultrasound,^[1] UV-IR light,^[2] or X-rays^[3]) provides an attractive alternative. However, quantification of the amount delivered remains a significant problem. First, calibration of the triggering beam can be difficult in complex systems (e.g., a living organism) because of the unknown and heterogenous nature of these systems. Second, the local concentration of inactive precursor may be unknown, which makes it difficult to deliver a specific concentration of substrate. One possible way to address this quantification problem relies on the simultaneous release of a reporter (in a one-to-one molar ratio) and the desired substrate from a common precursor. Quantitative analysis then can be done simply from analyzing the increase in the reporter signal after—or even better, during—activation at the targeted site.

Numerous caging groups have been introduced that allow release of the substrate following light activation of the caged precursors. Improvement of their photophysical and photochemical features has been extensively addressed.^[2] In contrast, optical reporting of uncaging has attracted much less

attention. Strategies relying on the concomitant release of a fluorophore were developed.^[4] These strategies used caging groups that were designed to release a fluorophore as a side product. However, efficient optical reporting of their release has remained limited to specific substrates. One way to overcome this limitation is to decouple the fluorescent reporter from the caging group. Herein, we adopt a modular approach in which photoactivation of a caged precursor leads to the release of not one, but two molecules: the desired substrate and the reporting fluorophore.

Our approach is based on a so-called “self-immolative” spacer.^[5] In these covalent chemical assemblies, commonly used for therapeutic or bioanalytical aims, a primary (e.g. enzymatic) reaction initiates internal molecular rearrangements driving a second reaction causing the release of a substrate (e.g. a drug or a probe). Self-immolative spacers uncouple the primary and the secondary reactions, which has made it possible to increase the diversity of enzyme substrates in prodrug strategies for targeted drug delivery.^[6] In addition, branched self-immolative spacers were recently shown to release two (or more) molecules after a single triggering cleavage.^[7] Thus we synthesized a caged, branched, self-immolative spacer to liberate the desired compound and fluorophore upon photoactivation (Scheme 1).



Scheme 1. A branched self-immolative spacer for uncaging with fluorescence reporting. Upon removal of a photolabile protecting group (circle), illumination initiates self-immolation leading to release of both the substrate (green ellipse) and the fluorophore (red square).

The usefulness of this strategy is governed by two main aspects: 1) the photochemical efficiency of the photolabile protecting group; 2) the stoichiometry and the kinetics for releasing the substrate and its fluorescent reporter. Herein, we did not attempt to optimize the photochemical step; thus, as a caging group, we used the 4,5-dimethoxy-2-nitrobenzyl moiety, which is widely used and acts also as a quencher (see below). In contrast, we designed the spacer to accelerate its self-immolation after photoactivation, as well as decrease the delay between the release of the substrate and its reporter (Scheme 2). We chose a 4,6-dibromo-2-hydroxy-5-methyl-1,3-

[*] Dr. R. Labruère, Dipl.-Chem. A. Alouane, S. Dubruille, Dr. F. Schmidt
 Institut Curie, Centre de Recherche
 26 rue d’Ulm, 75248 Paris (France)
 E-mail: frederic.schmidt@curie.fr

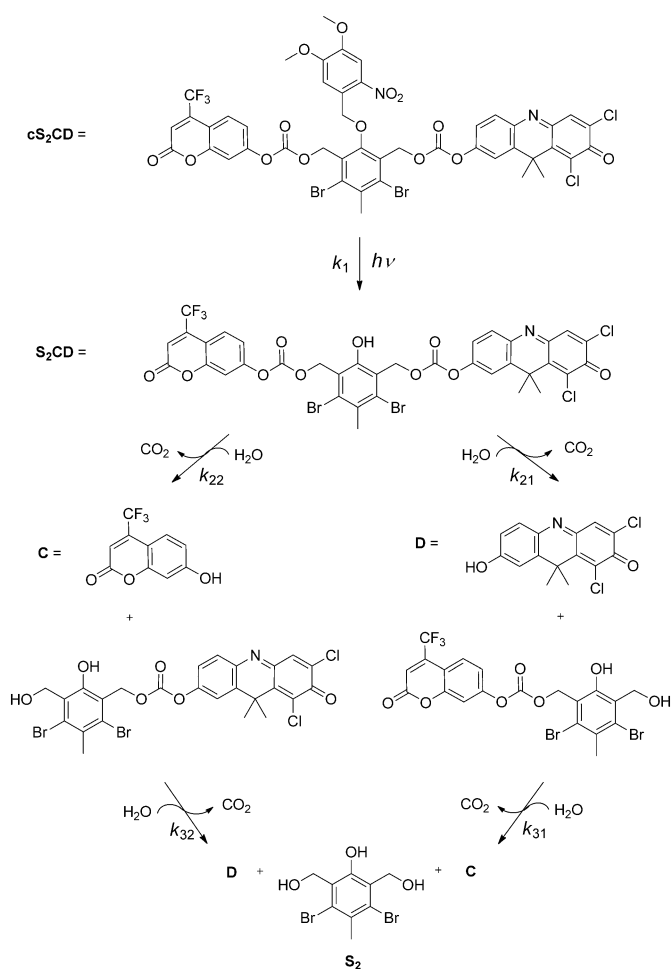
Dr. R. Labruère, Dipl.-Chem. A. Alouane, Dr. T. Le Saux, Dr. I. Aujard,
 Dr. A. Gautier, Prof. Dr. L. Jullien
 Ecole Normale Supérieure, Département de Chimie, UMR CNRS-
 ENS-UPMC 8640 PASTEUR
 24 rue Lhomond, 75231 Paris (France)
 E-mail: ludovic.jullien@ens.fr

Dr. R. Labruère, Dipl.-Chem. A. Alouane, S. Dubruille, Dr. F. Schmidt
 UMR 176
 26 rue d’Ulm, 75248 Paris (France)

Dr. P. Pelupessy
 Ecole Normale Supérieure, Département de Chimie, UMR CNRS-
 UPMC-ENS 7203 Laboratoire des Biomolécules
 24 rue Lhomond, 75231 Paris (France)

[**] This work has been supported by the ANR PCV 2008 (Proteophane) and ANR Blanc 2010 (Kituse).

Supporting information for this article (experimental details) is available on the WWW under <http://dx.doi.org/10.1002/anie.201204032>.



Scheme 2. Simplified kinetic scheme of self-immolation of the spacer cS_2CD . After cleavage of the photolabile protecting group, a cascade of internal reactions leads to the release of coumarin (**C**) and DDAO (**D**) fluorophores, which represent the desired substrate and reporter, together with carbon dioxide and the benzenic core S_2 .

phenylenedimethanol motif, which is predicted to self-immolate upon removal of the phenol group. Besides synthetic considerations, its symmetrical pattern of conjugated benzylic substituents should reduce the delay between the release of the desired product and the reporter fluorophore. Furthermore, to accelerate the reaction^[8] and make the release as substrate-independent as possible, we attached the benzylic positions of the spacer to the substrate/reporter moieties through carbonate linkages. To analyze the stoichiometry and the kinetics of self-immolation of the photoactivated spacer, we chose as a model substrate/reporter pair two fluorophores, whose emission is quenched and blue-shifted in the caged precursor with respect to the free state.

Hence we used coumarin (7-hydroxy-4-(trifluoromethyl)-coumarin, **C**) and DDAO (1,3-dichloro-9,9-dimethyl-9H-acridin-2(7)-one, **D**), which respectively exhibit strong emission in the blue and in the red regions only after ionization of their phenol group.^[9] These fluorophores absorb and emit in different wavelength ranges, which enabled us to separately investigate the temporal dependence of their release upon

uncaging, by recording fluorescence intensities at two emission wavelengths.^[4c-e]

The spacer cS_2CD was synthesized in five steps from 3,5-dibromo-4-methylphenol (see Scheme 2 and Supporting Information). Briefly, 4,6-dibromo-2-hydroxy-5-methyl-1,3-phenylene)dimethanol was obtained by bishydroxymethylation in 98% yield^[10] and its hydroxymethyl groups were protected with *tert*-butyldimethylsilyl groups (81% yield). The remaining phenol was subsequently alkylated with 4,5-dimethoxy-2-nitrobenzyl bromide (68% yield). After removal of the silyl protecting groups (60% yield), the bis(hydroxyethyl) intermediate was treated with phosgene followed by the fluorophores **C** and **D**, to afford cS_2CD in 33% yield. For kinetic analysis, we also synthesized 1) the symmetrical spacer cS_2D_2 incorporating two identical fluorophores **D** and 2) a model of our caged spacer in which one branch involved in self-immolation was removed (cS_1C). We anticipated that cS_1C would release **C** alone upon photoactivation (see Supporting Information, Chart S1).

First, stability and uncaging of cS_2CD were investigated in 1:1 mixture of acetonitrile/0.1M Britton–Robinson buffer pH 8 (*v/v*) at room temperature. We first showed that cS_2CD is stable in solution in the dark for 48 h, owing to the absence of a change in the absorption spectrum. Then we performed two series of UV-illumination experiments. To determine the molar ratio of the photo-induced release of **C** and **D**, we analyzed their concentrations by LC/MS after various durations of illumination at 365 nm. To analyze the self-immolation kinetics of cS_2CD , we then recorded the temporal change in the fluorescence intensity from a cS_2CD solution under continuous illumination at 365 nm.

Figure 1a displays the concentrations of **C** and **D** after illumination of duration τ , as determined by LC/MS analysis. As expected, their concentration increases with time and shows an exponential evolution (see Supporting Information, Section 2.2.3). Upon illuminating a $5.1 \pm 0.4 \mu M$ cS_2CD solution, we calculated $C_\infty = 5.3 \pm 0.5 \mu M$ and $D_\infty = 4.9 \pm 0.5 \mu M$ for the final concentrations of **C** and **D**, in agreement with a quantitative photoinduced release of both substrates. Furthermore, we also calculated from the global fit of cS_2CD uncaging a quantum yield $\phi(365 \text{ nm}) = 8.6 \pm 0.9 \times 10^{-4}$, in line with reported values for the *ortho*-nitrobenzyl caging group.^[11]

Figures 1b,c show the temporal evolutions of the fluorescence emissions $I_F^C(t)$ and $I_F^D(t)$ of **C** and **D**, respectively, upon continuous illumination of a $5.1 \pm 0.4 \mu M$ solution of cS_2CD at 298 K. Starting from a nonfluorescent cS_2CD solution, fluorescence emission increases, as anticipated, from photo-release of **C** and **D**. Again, the final signals demonstrated quantitative, equimolar photorelease of **C** and **D** from cS_2CD . Kinetic analysis of the experimental data must take into account the cascade of reactions involved in the self-immolation process (see Supporting Information, Section 2.2). We adopted the simplified kinetic Scheme shown in Scheme 2, which includes the steps typically occurring beyond the millisecond time scale.^[12] The caged precursor yields the phenol intermediate S_2CD , which subsequently disassembles along one of two pathways to give the same final products, a benzenic core S_2 together with **C** and **D**. In

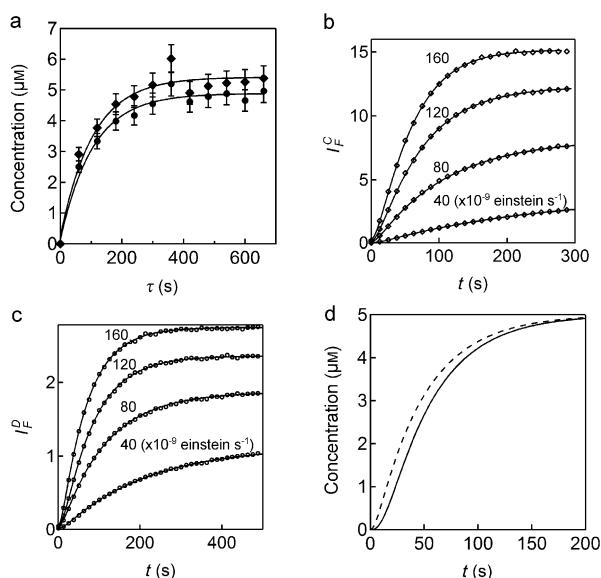


Figure 1. a) Photoreleased concentrations in **C** (◆) and **D** (●) after illumination for a duration τ of a $5.1 \mu\text{M}$ **cS₂CD** solution at 84×10^{-9} einstein s^{-1} light intensity. Solid line: fits of the data from Equations (34), (37) in the Supporting Information. b) Fluorescence emission of **C** $I_F^C(t)$ ($\lambda_{\text{em}} = 500$ nm) over time during illumination at $\lambda_{\text{exc}} = 365$ nm of a $5.1 \mu\text{M}$ **cS₂CD** solution at various light intensities ($40, 80, 120,$ and 160×10^{-9} einstein s^{-1}). Diamonds: experimental data; solid lines: fits from Equation (49) in the Supporting Information. c) Fluorescence emission of **D** $I_F^D(t)$ ($\lambda_{\text{em}} = 660$ nm) over time during illumination at $\lambda_{\text{exc},1} = 365$ nm and $\lambda_{\text{exc},2} = 645$ nm of a $5.1 \mu\text{M}$ **cS₂CD** solution at varying light intensities of $\lambda_{\text{exc},1}$ ($40, 80, 120,$ and 160×10^{-9} einstein s^{-1}). Circles: experimental data; solid lines: fits from Equation (50) in Supporting Information. d) Simulation of the change in concentration of **C** (solid line) and **D** (dashed line) over time upon continuous illumination of a $5 \mu\text{M}$ **cS₂CD** solution at 10^{-7} einstein s^{-1} light intensity, as obtained from Equations (46)–(48), (51), (52) using the values of $\epsilon\phi(365 \text{ nm})$, k_{21} , k_{22} , and k_{31} extracted from the fits. Solvent: 1:1 (v/v) $\text{CH}_3\text{CN}/0.1 \text{ M}$ Britton–Robinson buffer pH 8. $T = 298 \text{ K}$.

Scheme 2, the rate constant k_1 is associated with uncaging, whereas the rate constants k_{21} , k_{22} , k_{31} , and k_{32} all refer to the steps of self-immolation (see Supporting Information).

We obtained satisfactory fits of the kinetic data using $\phi(365 \text{ nm}) = 8.8 \pm 0.9 \times 10^{-4}$ for the **cS₂CD** uncaging quantum yield, $k_{21} = 0.10 \pm 0.02 \text{ s}^{-1}$, $k_{22} < 0.02 \text{ s}^{-1}$, and $k_{31} = 0.11 \pm 0.06 \text{ s}^{-1}$. To support our kinetic analysis, we first noted that the uncaging quantum yield $\phi(365 \text{ nm})$ was in line with the result calculated from the LC/MS analysis. The values of k_{21} and k_{31} were then compared with the values calculated from the analysis of self-immolation of the model **cS₁C** and **cS₂D₂** spacers (see Supporting Information, Section 2.2.1 and 2.2.2). A value for k_{21} of approximately 0.1 s^{-1} compares fairly well with the rate constant associated with the first **S₂D₂** self-immolation step (also approximately 0.1 s^{-1}). In fact, this result was as expected, because the same moiety **D** was first released from both **S₂CD** and **S₂D₂** phenols. We also saw an agreement between k_{31} (approximately 0.1 s^{-1}) and the rate constant for **cS₁C** self-immolation (approximately 0.3 s^{-1}). Indeed, these rate constants both corresponded to the

ultimate release of **C** in the self-immolation processes. Further evidence supporting our kinetic interpretation was found from analysis of the brightness of the intermediates involved in **S₂CD** self-immolation (see Supporting Information).

The preceding kinetic analysis makes it possible to evaluate the present strategy for uncaging with fluorescent reporting. The substrate and its reporter are released in a one-to-one molar ratio about ten seconds after removal of the phenol group. In fact, this time is among the shortest times ever reported for disassembly of a self-immolative linker.^[2h,13] Furthermore, using the values of the uncaging cross-section $\epsilon\phi(365 \text{ nm})$, where ϵ is the molar absorption coefficient, and the rate constants k_{21} , k_{22} , and k_{31} , we simulated the change in the concentrations of **C** and **D** upon illumination of a **cS₂CD** solution (see Figure 1 d). **C** is released about ten seconds after **D**. Although this delay would be detrimental to quantitative reporting of uncaging in an open system, it is sufficiently short to analyze most biological processes occurring in a closed system (e.g., a cell). Indeed the delay between the release of the substrate and its reporter remains moderate with respect to characteristic times of cellular events, many of which exceed the minute range (e.g., phosphorylation, protein translation, protein degradation).

Next, we reproduced the preceding uncaging experiments in human embryonic kidney (HEK) 293 cells. We incubated cells for 30 minutes in a solution of $5.3 \mu\text{M}$ **cS₂CD** in 100 mM PBS buffer pH 7.4. We observed identical cellular fluorescence following uncaging with 365 nm light when cells were incubated with $5 \mu\text{M}$ **cS₂CD** for 30 minutes or 2 hours (data not shown), suggesting that an incubation time of 30 min is sufficient to equilibrate the distribution of **cS₂CD** between the extracellular solution and the cytoplasm. After rinsing with PBS, cells were continuously illuminated at 365 nm and imaged in real time with epifluorescence microscopy using two independent channels, collecting the emission of **C** and **D** (see the Movie in the Supporting Information).^[14] We analyzed the kinetics of photoinduced release of **C** and **D** within HEK 293 cells (Supporting Information, Figure S8). We did not notice any difference in the uncaging behavior among cells that were similarly illuminated. Proceeding as above, we calculated $\phi(365 \text{ nm}) = 3.5 \pm 0.2 \times 10^{-4}$, $k_{21} \approx 0.2 \text{ s}^{-1}$, and $k_{31} \approx 0.1 \text{ s}^{-1}$ in good agreement with the values found in vitro, showing no significant alteration of the rate constants associated with **cS₂CD** photoactivation in living cells.

Finally, we used confocal microscopy to analyze the final concentrations of **C** and **D** within the cells after uncaging with 365 nm light. Excitation at 405 nm and 633 nm light were subsequently used to image **C** and **D** under optimized conditions. Figures 2 a–c show confocal micrographs of non-illuminated **cS₂CD**-incubated control cells. Under these imaging conditions, some auto-fluorescence was observed in the green emission channel upon exciting at 405 nm (Figure 2 b). In contrast, no significant auto-fluorescence was observed in the far-red emission channel with 633 nm light excitation (Figure 2 c). Figures 2 d, e show confocal micrographs of **cS₂CD**-incubated cells that were exposed to 365 nm light until a steady state of fluorescence was achieved. We

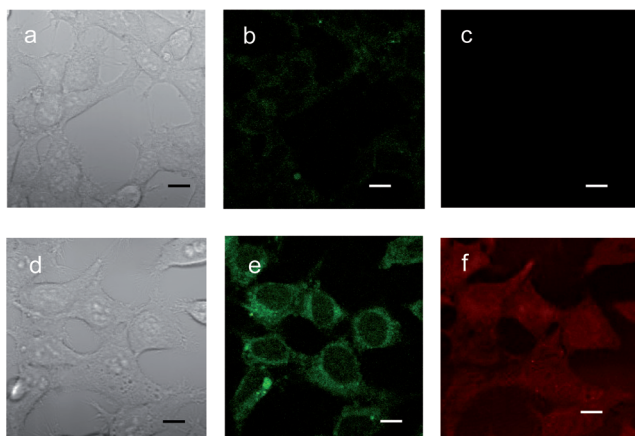


Figure 2. Confocal micrographs of HEK 293 cells incubated with $5.3 \mu\text{M}$ cS_2CD before (a–c) and after irradiation at 365 nm for 80 s (d–f). a, d) Transmission, b, e) green fluorescence emission with excitation at $\lambda_{\text{exc}} = 405 \text{ nm}$ (emission of **C**), and c, f) far-red fluorescence emission with excitation at $\lambda_{\text{exc}} = 633 \text{ nm}$ (emission of **D**). Buffer: 100 mM PBS pH 7.4 with 1% DMSO. $T = 298 \text{ K}$. Scale bar = $8 \mu\text{m}$.

observed strong green and far-red fluorescence emission from these cells, which demonstrated the release of **C** and **D**.

We noticed that fluorescence levels remained constant for more than two hours, showing the absence of any significant fluorophore leakage over the time scale of our uncaging experiments (data not shown). Then we calibrated the fluorescence signal using standard solutions of **C** and **D**, to convert the fluorescence signals in concentrations. We averaged five cells located in similarly illuminated regions and found final concentrations of $C_{\infty} = 5.4 \pm 0.5 \mu\text{M}$ and $D_{\infty} = 4.8 \pm 0.5 \mu\text{M}$. This result suggests that the cytoplasmic concentration of cS_2CD was approximately equal to the extracellular solution. Moreover, it shows that both fluorophores are quantitatively released in a one-to-one molar ratio in living cells, as was also shown in vitro.

In conclusion, we introduced a caged, branched, self-immolative spacer that allows us to efficiently release a desired substrate and a fluorescent reporter, in a one-to-one molar ratio, by illuminating with light. The kinetics of disassembly have been thoroughly analyzed in vitro and in cells. Both the substrate and its reporter are released rapidly and simultaneously enough to consider this caged platform with fluorescence reporting sufficient for various biological applications. In particular, this versatile approach is compatible with optimizing the photophysical and photochemical characteristics of the caging group and its fluorescent reporter. Furthermore, the present modular design could be adapted to other triggering and reporting agents, making this self-immolative spacer attractive for a wide range of applications.

Received: May 24, 2012

Published online: ■ ■ ■ ■ ■, ■ ■ ■ ■ ■

Keywords: caging groups · fluorescence · imaging agents · kinetics · self-immolative spacers

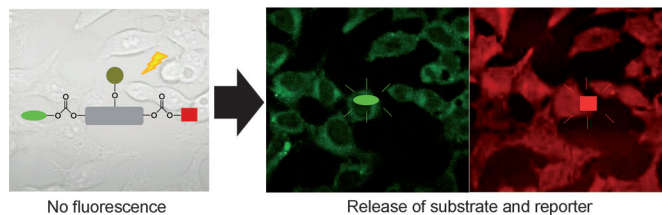
- [1] O. Couture, M. Faivre, N. Pannacci, A. Babataheri, V. Servois, P. Tabeling, M. Tanter, *Med. Phys.* **2011**, *38*, 1116–1123.
- [2] For recent reviews, see: a) *Dynamic studies in biology* (Eds.: M. Goeldner, R. Givens), Wiley-VCH, Weinheim, **2005**; b) G. Mayer, A. Heckel, *Angew. Chem.* **2006**, *118*, 5020–5042; *Angew. Chem. Int. Ed.* **2006**, *45*, 4900–4921; c) G. C. R. Ellis-Davies, *Nat. Methods* **2007**, *4*, 619–628; d) D. D. Young, A. Deiters, *Org. Biomol. Chem.* **2007**, *5*, 999–1005; e) H.-M. Lee, D. R. Larson, D. S. Lawrence, *ACS Chem. Biol.* **2009**, *4*, 409–427; f) A. Specht, F. Bolze, Z. Omran, J.-F. Nicoud, M. Goeldner, *HFSP J.* **2009**, *3*, 255–264; g) H. Yu, J. Li, D. Wu, Z. Qiu, Y. Zhang, *Chem. Soc. Rev.* **2010**, *39*, 464–473; h) A. Deiters, *ChemBioChem* **2010**, *11*, 47–53.
- [3] M. Petit, G. Bort, B.-T. Doan, C. Sicard, D. Ogden, D. Scherman, C. Ferroud, P. I. Dalko, *Angew. Chem.* **2011**, *123*, 9882–9885; *Angew. Chem. Int. Ed.* **2011**, *50*, 9708–9711.
- [4] a) V. Hagen, S. Frings, J. Bendig, D. Lorenz, B. Wiesner, U. B. Kaupp, *Angew. Chem.* **2002**, *114*, 3775–3777; *Angew. Chem. Int. Ed.* **2002**, *41*, 3625–3628; b) J. R. R. Majjigapu, A. N. Kurchan, R. Kottani, T. P. Gustafson, A. G. Kutateladze, *J. Am. Chem. Soc.* **2005**, *127*, 12458–12459; c) N. Gagey, P. Neveu, L. Jullien, *Angew. Chem.* **2007**, *119*, 2519–2521; *Angew. Chem. Int. Ed.* **2007**, *46*, 2467–2469; d) N. Gagey, P. Neveu, C. Benbrahim, B. Goetz, I. Aujard, J.-B. Baudin, L. Jullien, *J. Am. Chem. Soc.* **2007**, *129*, 9986–9998; e) N. Gagey, M. Emond, P. Neveu, C. Benbrahim, B. Goetz, I. Aujard, J.-B. Baudin, L. Jullien, *Org. Lett.* **2008**, *10*, 2341–2344.
- [5] C. A. Blencowe, A. T. Russell, F. Greco, W. Hayes, D. W. Thornthwaite, *Polym. Chem.* **2011**, *2*, 773–790.
- [6] O. Redy, E. Kisin-Finifer, E. Sella, D. Shabat, *Org. Biomol. Chem.* **2012**, *10*, 710–715.
- [7] a) F. M. H. de Groot, C. Albrecht, R. Koekkoek, P. H. Beusker, H. W. Scheeren, *Angew. Chem.* **2003**, *115*, 4628–4632; *Angew. Chem. Int. Ed.* **2003**, *42*, 4490–4494; b) R. J. Amir, N. Pessah, M. Shamis, D. Shabat, *Angew. Chem.* **2003**, *115*, 4632–4637; *Angew. Chem. Int. Ed.* **2003**, *42*, 4494–4499; c) M. L. Szalai, R. M. Kewitch, D. V. McGrath, *J. Am. Chem. Soc.* **2003**, *125*, 15688–15689.
- [8] H. Y. Lee, X. Jiang, D. Lee, *Org. Lett.* **2009**, *11*, 2065–2068.
- [9] a) P. F. Corey, R. W. Trimmer, W. G. Biddlecom, *Angew. Chem.* **1991**, *103*, 1694–1696; *Angew. Chem. Int. Ed. Eng.* **1991**, *30*, 1646–1648; b) J.-A. Richard, Y. Meyer, V. Jolivel, M. Massonneau, R. Dumeunier, D. Vaudry, H. Vaudry, P.-Y. Renard, A. Romieu, *Bioconjugate Chem.* **2008**, *19*, 1707–1718; c) D. Warther, F. Bolze, J. Lonéard, S. Gug, A. Specht, D. Puliti, X.-H. Sun, P. Kessler, Y. Lutz, J.-L. Vonesch, B. Winsor, J.-F. Nicoud, M. Goeldner, *J. Am. Chem. Soc.* **2010**, *132*, 2585–2590.
- [10] M. Kohn, M. Weissberg, *Monatsh. Chem.* **1924**, *45*, 295–303.
- [11] I. Aujard, C. Benbrahim, M. Gouget, O. Ruel, J.-B. Baudin, P. Neveu, L. Jullien, *Chem. Eur. J.* **2006**, *12*, 6865–6879.
- [12] a) C. K. Sauers, W. P. Jencks, S. Groh, *J. Am. Chem. Soc.* **1975**, *97*, 5546–5553; b) J. Zhao, T. D. Gover, S. Muralidharan, D. A. Auston, D. Weinreich, J. P. Y. Kao, *Biochemistry* **2006**, *45*, 4915–4926.
- [13] a) I. E. Sella, A. Lubelski, J. Klaffer, D. Shabat, *J. Am. Chem. Soc.* **2010**, *132*, 3945–3952; b) R. E. Wang, F. Costanza, Y. Niu, H. Wu, Y. Hu, W. Hang, Y. Sun, J. Cai, *J. Controlled Release* **2012**, *159*, 154–163.
- [14] a) K. Zrelli, T. Barilero, E. Cavatore, H. Berthoumieux, T. Le Saux, V. Croquette, A. Lemarchand, C. Gosse, L. Jullien, *Anal. Chem.* **2011**, *83*, 2476–2484; b) T. Barilero, T. Le Saux, C. Gosse, L. Jullien, *Anal. Chem.* **2009**, *81*, 7988–8000.

Communications

Chemical Biology

R. Labruère, A. Alouane, T. Le Saux,
I. Aujard, P. Pelupessy, A. Gautier,
S. Dubruille, F. Schmidt,*
L. Jullien* _____ ■■■■-■■■■

“Self-Immolative” Spacer for Uncaging
with Fluorescence Reporting



Dual photoliberation: A caged, branched, self-immolative spacer (see scheme, gray box) was designed to rapidly and simultaneously release a desired compound (green) and a fluorophore (red) upon

photoactivation. Careful kinetic analysis of the disassembly of the spacer shows that it occurs on the shortest time scale yet reported.